



NAVAL POSTGRADUATE SCHOOL

MONTEREY, CALIFORNIA

THESIS

Z-M IN LIGHTNING FORECASTING

by

Alexia J. Machina

March 2009

Thesis Advisor:
Second Reader:

Wendell A. Nuss
Karl D. Pfeiffer

Approved for public release; distribution is unlimited.

THIS PAGE INTENTIONALLY LEFT BLANK

REPORT DOCUMENTATION PAGE			<i>Form Approved OMB No. 0704-0188</i>	
Public reporting burden for this collection of information is estimated to average 1 hour per response, including the time for reviewing instruction, searching existing data sources, gathering and maintaining the data needed, and completing and reviewing the collection of information. Send comments regarding this burden estimate or any other aspect of this collection of information, including suggestions for reducing this burden, to Washington headquarters Services, Directorate for Information Operations and Reports, 1215 Jefferson Davis Highway, Suite 1204, Arlington, VA 22202-4302, and to the Office of Management and Budget, Paperwork Reduction Project (0704-0188) Washington DC 20503.				
1. AGENCY USE ONLY (Leave blank)		2. REPORT DATE March 2009	3. REPORT TYPE AND DATES COVERED Master's Thesis	
4. TITLE AND SUBTITLE Z-M in Lightning Forecasting			5. FUNDING NUMBERS	
6. AUTHOR(S) Alexia J. Machina				
7. PERFORMING ORGANIZATION NAME(S) AND ADDRESS(ES) Naval Postgraduate School Monterey, CA 93943-5000			8. PERFORMING ORGANIZATION REPORT NUMBER	
9. SPONSORING /MONITORING AGENCY NAME(S) AND ADDRESS(ES) N/A			10. SPONSORING/MONITORING AGENCY REPORT NUMBER	
11. SUPPLEMENTARY NOTES The views expressed in this thesis are those of the author and do not reflect the official policy or position of the Department of Defense or the U.S. Government.				
12a. DISTRIBUTION / AVAILABILITY STATEMENT Approved for public release; distribution is unlimited.			12b. DISTRIBUTION CODE	
13. ABSTRACT (maximum 200 words) Frozen hydrometeors are required for a storm to produce lightning. Previous research has made strong correlations between ice mass and lightning flash rate and lightning flash density. This study attempted to correlate ice mass to lightning potential Operational interest is centered at Cape Canaveral Air Force Station/Kennedy Space Center where accurate weather forecasting is vital to mission requirements, resource protection, and personnel safety. Four pulse storms were chosen for the study: 2 June 2004, 26 June 2004, 6 June 2005, and 15 June 2005. These storms were known lightning producers. The ice mass of each storm was calculated using a new layered approach called Layered Vertically Integrated Frozen Content (LVIF). The LVIF technique uses radar reflectivity (Z) to calculate ice content (M) at six temperature layers between -10°C and -40°C, with each layer 5°C. This Z-M relationship was analyzed for lightning potential. The results indicate there is no correlation between LVIF and lightning potential.				
14. SUBJECT TERMS Lightning, Ice content, Florida			15. NUMBER OF PAGES 61	
			16. PRICE CODE	
17. SECURITY CLASSIFICATION OF REPORT Unclassified	18. SECURITY CLASSIFICATION OF THIS PAGE Unclassified	19. SECURITY CLASSIFICATION OF ABSTRACT Unclassified	20. LIMITATION OF ABSTRACT UU	

THIS PAGE INTENTIONALLY LEFT BLANK

Approved for public release; distribution is unlimited.

Z-M IN LIGHTNING FORECASTING

Alexia J. Machina
Captain, United States Air Force
B.S., United States Air Force Academy, 2003

Submitted in partial fulfillment of the
requirements for the degree of

MASTER OF SCIENCE IN METEOROLOGY

from the

**NAVAL POSTGRADUATE SCHOOL
March 2009**

Author: Alexia J. Machina

Approved by: Wendell A. Nuss
Thesis Advisor

Karl D. Pfeiffer
Second Reader

Philip A. Durkee
Chairman, Department of Meteorology

THIS PAGE INTENTIONALLY LEFT BLANK

ABSTRACT

Frozen hydrometeors are required for a storm to produce lightning. Previous research has made strong correlations between ice mass and lightning flash rate and lightning flash density. This study attempted to correlate ice mass to lightning potential. Operational interest is centered at Cape Canaveral Air Force Station/Kennedy Space Center where accurate weather forecasting is vital to mission requirements, resource protection, and personnel safety.

Four pulse storms were chosen for the study: 2 June 2004, 26 June 2004, 6 June 2005, and 15 June 2005. These storms were known lightning producers. The ice mass of each storm was calculated using a new layered approach called Layered Vertically Integrated Frozen Content (LVIF). The LVIF technique uses radar reflectivity (Z) to calculate ice content (M) at six temperature layers between -10°C and -40°C, with each layer 5°C. This Z-M relationship was analyzed for lightning potential. The results indicate there is no correlation between LVIF and lightning potential.

THIS PAGE INTENTIONALLY LEFT BLANK

TABLE OF CONTENTS

I.	INTRODUCTION.....	1
A.	FLORIDA CLIMATE.....	2
B.	OPERATIONAL MOTIVATION.....	3
C.	LAYERED VERTICALLY INTEGRATED LIQUID METHOD.....	4
D.	DEVELOPING LAYERED VERTICALLY INTEGRATED FROZEN CONTENT.....	5
1.	Equations.....	5
2.	Choosing the LVIF Layers.....	7
E.	LIMITATIONS/GOALS.....	8
II.	DATA.....	11
A.	STORM DATABASE.....	11
B.	RADAR.....	12
C.	LIGHTNING.....	12
D.	SOUNDING DATA.....	12
E.	CHOSEN EVENTS.....	13
1.	2 June 2004.....	13
2.	26 June 2004.....	14
3.	6 June 2005.....	14
4.	15 June 2005.....	15
III.	METHODS.....	17
A.	RADAR.....	17
1.	Reflectivity.....	17
2.	Height.....	18
B.	LIGHTNING.....	20
C.	LVIF CALCULATIONS.....	21
1.	Vertical Plot.....	21
2.	Ice Mass.....	24
IV.	RESULTS.....	25
A.	LVIF RESULTS.....	25
1.	2 June 2004.....	25
2.	26 June 2004.....	27
3.	6 June 2005.....	28
4.	15 June 2005.....	30
5.	Comparison of all Storms.....	31
V.	CONCLUSIONS AND RECOMMENDATIONS.....	35
A.	GOALS ACCOMPLISHED.....	35
1.	Data Handling.....	35
2.	Calculate LVIF.....	35
3.	LVIF Relationship to Lightning.....	36
4.	Lightning Forecast Potential.....	37

VI.	DISCUSSION	39
A.	SOURCES OF ERROR.....	39
1.	Data	39
a.	<i>Lightning Data</i>	39
b.	<i>Missing Data</i>	39
2.	Calculations	40
B.	FUTURE RESEARCH.....	41
	LIST OF REFERENCES	43
	INITIAL DISTRIBUTION LIST	45

LIST OF FIGURES

Figure 1.	a. Mean Annual cloud-to-ground flash density for the U.S, 1989-1996. [From Huffines and Orville (1999)] b. Mean Annual cloud-to-ground flash density for Florida, 1986-1995. [From Hodanish et al. (1997)].....	2
Figure 2.	Locations of all storm boxes relative to one another and to the radar.	13
Figure 3.	Sample of the reflectivity grid taken from 2 June 2004, elevation angle 0.5°. The boxed area indicates the storm location.	18
Figure 4.	Discrepancies with height between two scans at the same elevation angle (0.5°).	19
Figure 5.	Distance from the radar to the storm versus height.	20
Figure 6.	Example from 2 June 2004: a. Elevation Angle 5.2°; b. Elevation Angle 8.7°.	22
Figure 7.	Sample Reflectivity with Height Spline plot from 2 June 2004.	23
Figure 8.	a. Total LVIF for 2 June 2004. b. LVIF of each thermal layer for 2 June 2004.....	26
Figure 9.	a. Total LVIF for 26 June 2004. b. LVIF of each thermal layer for 26 June 2004.....	28
Figure 10.	a. Total LVIF for 6 June 2005. b. LVIF of each thermal layer for 6 June 2005.....	29
Figure 11.	a. Total LVIF for 15 June 2005. b. LVIF of each thermal layer for 15 June 2005.....	31
Figure 12.	a. Total LVIF for all the storms. b. Reflectivity averages for all the storms ..	33
Figure 13.	Differences between Height used and Actual Height. Height differences greater than zero are an under estimate for the height used. Height differences less than zero are an over estimate for the height used.	41

THIS PAGE INTENTIONALLY LEFT BLANK

LIST OF TABLES

Table 1.	Table of calculations	7
----------	-----------------------------	---

THIS PAGE INTENTIONALLY LEFT BLANK

ACKNOWLEDGMENTS

I would like to thank the following people for their help and support: Professor Wendell Nuss for his guidance during my thesis as well as scripting my radar code; Mary Jordan for spending hours working on recreating the radar data in MATLAB and answering countless questions; Lt Col. Karl Pfeiffer for filling in as my second reader; and William Roeder for suggesting this topic, providing storm data, and several background articles.

THIS PAGE INTENTIONALLY LEFT BLANK

I. INTRODUCTION

Lightning only occurs when certain atmospheric criteria are satisfied. It is dependent on three things: 1) a convective updraft that is able to support mixed-phase precipitation ice processes; and 2) graupel-ice crystal collisions in the presence of super-cooled water; and 3) particle charge separation (Gauthier et al. 2006). Takahashi (1978) states that within the updraft column, graupel will be electrified by collision with ice crystals. The electrification of the atmosphere is either an inductive or non-inductive process (Kuettner et al. 1981). In a non-inductive process, electro-chemical or thermoelectric properties of colliding solid and liquid hydrometers create a charge separation. Inductive processes rely on a preexisting external electric field to induce charges on polarized particles, which subsequently are segregated through collision and separation (Kuettner et al. 1981). Kuettner et al. (1981) found that the non-inductive mechanism controls the charge distribution and its polarity and the inductive mechanism controls the field strength. Takahashi's (1978) laboratory results found that the magnitude and sign of the electrification is highly dependent on the temperature and cloud water content.

Temperature and cloud water content are variables that can be observed at the operational level. The electric field is an elusive parameter for a forecaster and can only be observed using aircraft measurements. This is done in a research capacity, such as in Dye and Willett (2007) who recorded the electric field in Florida anvils using an airborne field mill system. However, operationally, a forecaster cannot measure/observe the electrical field except with the occurrence of lightning. Therefore, radar and balloon data are the best alternatives for identifying lightning precursors. Both forecast and observed Skew Ts are used to identify the freezing level(s) within the temperature profile. Radar is used in numerous ways in thunderstorm forecasting to track the movement, intensity, structure, and height of the storm.

Since ice is fundamental to lightning production, the purpose of this study is to relate lightning occurrence to a trend of frozen content in storms. This study will be focused on lightning producing storms over Florida and will extract the ice content from

radar data using a Z-M relationship. The Z-M relationship documented by Carey and Rutledge (2000) correlates radar reflectivity (Z) and ice concentration (M). Using storms that are known lightning producers confirms the presence of the necessary atmospheric conditions for lightning, specifically the electric field, charge separation and polarity. Therefore, the focus of the study can be on the presence of frozen hydrometers.

A. FLORIDA CLIMATE

Florida is often referred to as the lightning capital of the United States (Hodanish et al. 1997) or Lightning Alley (Lambert et al. 2007). This title comes from the lightning frequency which is determined using flash density (flashes $\text{km}^{-2} \text{ year}^{-1}$). The maximum flash density (greater than 11 flashes $\text{km}^{-2} \text{ year}^{-1}$) in the United States is over Central Florida (Figure 1).

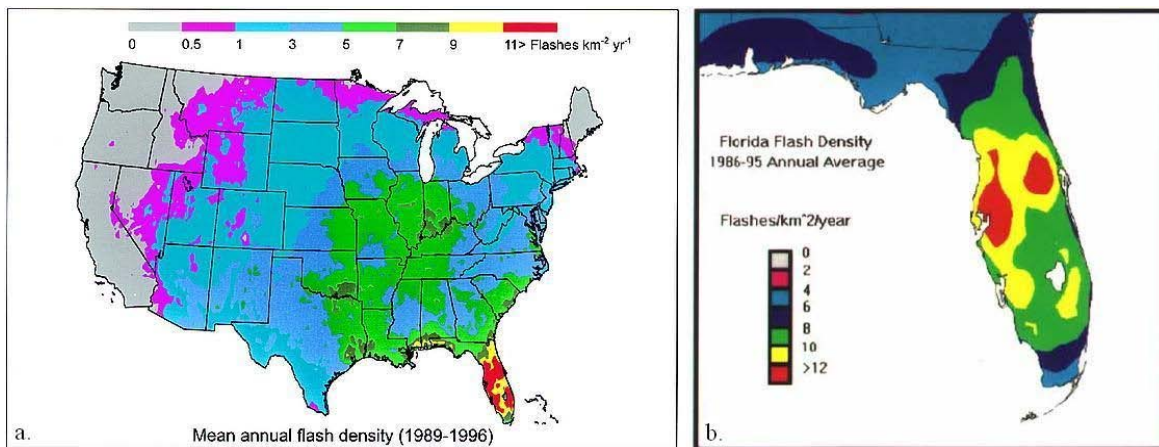


Figure 1. a. Mean Annual cloud-to-ground flash density for the U.S, 1989-1996. [From Huffines and Orville (1999)] b. Mean Annual cloud-to-ground flash density for Florida, 1986-1995. [From Hodanish et al. (1997)]

At first glance, the national map (Figure 1a) depicts a more severe picture of Florida's annual lightning than the state map (Figure 1b). However, upon closer examination the two maps are quite similar. Huffines and Orville (1999) used an upper limit for maximum flash density of greater than 11 flashes $\text{km}^{-2} \text{ year}^{-1}$, whereas Hodanish et al. (1997) used greater than 12 flashes $\text{km}^{-2} \text{ year}^{-1}$, which reduces maxima regions. Differences could also be due to the grid resolution. Huffines and Orville's (1999) map used a grid size that was 22 km to the north-south direction and 18 km in the

east-west direction; whereas Hodanish et al. (1997) used 14 km and 21 km, respectively. Regardless of the slight differences in the maxima locations, Florida is undeniably the most active lightning region in the country.

Within Florida, east-central and west-central are the regions of maximum annual lightning. Florida's thunderstorm activity can be attributed to a number of things to include: differential heating, water-land distributions, dying fronts, stationary boundaries, tropical cyclones, and the sea breeze. The summer time, defined by Hodanish et al. (1997) as June to September, is the most active season and directly related to the seasonal weather patterns. Land/Sea breezes from the Atlantic Ocean and the Gulf of Mexico contribute to the numerous thunderstorms. Low level convergence is maximized over Central Florida where the sea breezes from the east and west meet. The combination of available moisture and daytime heating, produce severe thunderstorms with hail, wind, and lightning.

B. OPERATIONAL MOTIVATION

In addition to being a lightning hot spot, east Central Florida is also home to Cape Canaveral Air Force Station/Kennedy Space Center (CCAFS/KSC), the National Aeronautics and Space Administration's (NASA) space vehicle launch facility and launch control center. Accurate weather forecasting is vital to CCAFS/KSC operations as numerous weather phenomenon affect the mission launch capability, to include: upper level winds, hail, and lightning. Tailored weather support for CCAFS/KSC is provided by the 45 Weather Squadron (WS) on Patrick Air Force Base (AFB) for personnel safety, resource protection, pre-launch ground processing, day-of-launch, post-launch, and special operations (Roeder et al. 2005). From 1988 to 2005, weather was a factor in over one-third of all delayed launches (48 of 136) and almost half of the scrubbed missions (105 of 216) (Roeder et al. 2005). The 45 WS is equipped with a state of the art lightning detection system, custom radar configurations, and an elaborate lightning watches/warnings policy.

Ideally, a forecaster would like to identify lightning warning signs in the atmospheric profile with a lead time of greater than 30 minutes. In order to provide ample resource protection, the 45 WS has developed a unique and highly refined lightning watch and warning system. Using 13 points of operational interest, a five nautical mile ring encircles each point (Weems et al. 2001). Lightning within five nautical miles of any point of interest triggers a lightning watch for that ring. A lightning warning is initiated when lightning is imminent or occurring within five nautical miles of any point. This study hopes to aid lightning forecasting by developing parameters based on precursor conditions as opposed to waiting for the lightning to occur somewhere else first.

C. LAYERED VERTICALLY INTEGRATED LIQUID METHOD

As previously stated, Takahashi (1978) found that the magnitude and sign of the electrification depends on the temperature and cloud water content. Radar has been used for over 30 years to calculate cloud water content. Originally developed by Greene and Clark (1972), the more commonly recognized vertically integrated liquid (VIL) calculates the liquid content for the entire atmospheric column using radar reflectivity. Subsequent to Greene and Clark's initial research, VIL has been adopted as a standard radar product and is often used as an indicator for severe weather. VIL has applications for lightning forecasting since it indicates the potential for severe weather. Higher VIL indicates a larger mixed phase which is required for lightning. Because the presence of supercooled drops is required for lightning (Gauthier et al. 2006), the 45 WS used VIL-above 0°C prior to 2001 as an indicator of lightning potential (Weems et al. 2001).

In 2001, the 45 WS adopted a new technique, layered vertically integrated liquid (LVIL), which was tested in a thesis by D'Arcangelo (2000). Ultimately, both LVIL and VIL-above 0°C have the same goal: to isolate the ideal region for lightning production. D'Arcangelo (2000) developed the LVIL techniques by modifying the VIL-above 0°C. LVIL out performed VIL-above-0°C in a skill score test that weighted probability of

detection, a Kuipers skill score, and false alarm rate. (The Kuipers skill score represents skill over a random forecast.) The layered approach more accurately isolates the region of the atmosphere critical to lightning production.

In LVIL, the atmosphere is subdivided into four thermal layers between 0°C and -20°C with each layer having a 5°C thickness. D’Arcangelo (2000) found the two layers, -10° to -15°C and -15°C to -20°C, are the ideal region for forecasting lightning onset. D’Arcangelo used Greene and Clark’s equation (1972):

$$LVIL = \sum 3.44 \times 10^{-6} \left[\left(\frac{Z_i + Z_{i+1}}{2} \right) \right]^{4/7} dh \quad (1)$$

where Z_i and Z_{i+1} are radar reflectivities in mm^6m^{-3} for the upper and lower temperature levels and dh is the thickness of the layer. The constant, 3.44×10^{-6} , is a derivative of the Marshall-Palmer (M-P) drop size distribution (Marshall and Palmer 1948) which encompasses the rain rate, drop density, and drop distribution.

D. DEVELOPING LAYERED VERTICALLY INTEGRATED FROZEN CONTENT

Ice is one of the key ingredients for lightning to occur which means that identifying the frozen content has the potential for being a better indicator of lightning onset. Graupel mass and mixed-phase processes are well correlated to lightning. Using D’Arcangelo’s (2000) thesis as a motivation, this study will adapt the LVIL concept to test an algorithm for layered vertically integrated frozen (LVIF) water content. Due to the success of the LVIL, a layered approach to the VIF is suggested to be better than total VIF.

1. Equations

The first step in developing a LVIF requires a correlation between the radar reflectivity (Z) and the ice water content or ice mass (M_{ice}). Carey and Rutledge (2000) first developed an equation while studying tropical convection:

$$M_{ICE} = 1000\pi \left(\frac{\rho_i}{\rho_a} \right) N_0^{\frac{3}{7}} \left(\frac{5.28 \times 10^{-18}}{720} Z_H^{ICE} \right)^{\frac{4}{7}} \quad (2)$$

where ρ_i is the density of ice at 0°C and ρ_a is air density, N_0 is the intercept parameter for an inverse exponential distribution of ice, and Z_H^{ICE} is horizontal reflectivity of ice in mm^6m^{-3} . Both LVIL and LVIF require reflectivity (Z) to be converted from dBZ to mm^6m^{-3} . The unit conversion, obtained from Rinehart (1997) is as follows:

$$Z_{\text{mm}^6/\text{m}^3} = 10^{\frac{Z_{\text{dBZ}}}{10}} \quad (3)$$

The original Carey and Rutledge (2000) experiment used a polarimetric radar to extract the Z_H^{ICE} values. This study will use radar data from Melbourne, FL (KMLB) which operates a non-polarized radar platform. Since a polarimetric radar is not available, it is impossible to calculate the Z_H^{ICE} and instead the radar reflectivity (Z) must be used. This simplification was also used in Gauthier et al. (2006), where they used archived radar data and applied (2) in a secondary form:

$$M_{ICE} = 1000\pi(\rho_i)N_0^{\frac{3}{7}}\left(\frac{5.28 \times 10^{-18}}{720}Z\right)^{\frac{4}{7}} \quad (4)$$

One discrepancy between these Z-M calculations was identified. In the Carey and Rutledge (2000) paper they used $\rho_i = 0.917 \text{ kg/m}^3$, however, in subsequent articles (Peterson and Rutledge 2001; Gauthier et al. 2006) $\rho_i = 917 \text{ kg/m}^3$. To remain consistent, since this study uses (4) from Gauthier et al. (2006) and not (2) from Carey and Rutledge (2000), $\rho_i = 917 \text{ kg/m}^3$ will be used. The intercept parameter N_0 is unchanged from the Carey and Rutledge (2000) study, where $N_0 = 4 \times 10^{-6} \text{ m}^{-4}$ (derived from the bulk-microphysical parameter for tropical convection over the Tiwi Islands). Since the KMLB radar and all the studied storms are south of 30°N, a generic cut off for the tropics, the same N_0 value will be used. Hodanish et al. (1997) describes Florida as a near-tropical climate. Furthermore, Gauthier et al. (2006) used (4) while studying storms in Houston, TX which is higher in latitude than KMLB. According to Carey and Rutledge (2000), the constants in (2) and repeated in (4), are derived from the Rayleigh scattering expressions for reflectivity and ice. Doviak and Zrnić (1993) provide further clarification and it is understood that the constants include approximations for drop

volume diameter, rain rate, and forward scattering. Further calculations to determine a better or different constant are beyond the scope of this study. No alterations will be made.

The following table summarizes the equations that are used in the LVIL versus the LVIF calculations:

Comparison of Calculations between LVIL and LVIF		
	LVIL Calculations	LVIF Calculations
1	$M = \frac{\pi(\rho_w)N_0}{(720 \times 10^{18} N_0)^{\frac{4}{7}}} (Z)^{\frac{4}{7}}$ <p style="text-align: center;">or</p> $M = \pi(\rho_w)N_0^{\frac{3}{7}} \left(\frac{10^{-18}}{720} Z\right)^{\frac{4}{7}}$	$M_{ICE} = 1000\pi(\rho_i)N_0^{\frac{3}{7}} \left(\frac{5.28 \times 10^{-18}}{720} Z\right)^{\frac{4}{7}}$
2	$N_0 = 8 \times 10^{-6} \text{ m}^{-4}, \rho_w = 10^6 \text{ g/m}^3$	$N_0 = 4 \times 10^{-6} \text{ m}^{-4}, \rho_i = 917 \text{ kg/m}^3$
3	$M = 3.44 \times 10^{-3} Z^{\frac{4}{7}}$	$M_{ICE} = 6.0734 \times 10^{-3} Z^{\frac{4}{7}}$
4	$M^* = 3.44 \times 10^{-6} \int_{hbase}^{htop} Z^{\frac{4}{7}} dh$	$M^* = 6.0734 \times 10^{-3} \int_{hbase}^{htop} Z^{\frac{4}{7}} dh$
5	$LVIL = \sum 3.44 \times 10^{-6} \left[\left(\frac{Z_i + Z_{i+1}}{2}\right)\right]^{4/7} dh$	$LVIF = \sum 6.0734 \times 10^{-3} \left[\left(\frac{Z_i + Z_{i+1}}{2}\right)\right]^{4/7} dh$
6	Units of LVIL: kg/m ²	Units of LVIF: g/m ²

Table 1. Table of calculations

This table highlights the prominent differences and similarities between LVIL and LVIF. Row one is the starting format of the Z-M relationships, described above as equation (4). The constants used are listed in row two. The equations from row one with the constant substituted are shown in row three. The integration from the base of the layer to the top of the layer is in row four. Finally, row five is final layered vertically integrated equations, described above for LVIL as equation (1). Row six is the units for LVIL and LVIF.

2. Choosing the LVIF Layers

Similar to the LVIL technique, LVIF requires a temperature profile to isolate the region of the atmosphere most favorable for ice formation, charge separation, and

lightning onset. Takahashi (1978) hypothesized that higher electrification occurs in the lower temperature region of the cloud where there are a greater number of ice crystals. Takahashi (1978) cites previous works that recommend a temperature range of 0°C to -40°C. Carey and Rutledge (2000) also used 0°C to -40°C for the range of mixed phase graupel mass. They found that for tropical convection supercooled drops are present in the 0 to -10°C layer and above -10°C is the most likely region for frozen drops or graupel. In the Gauthier et al. (2006) Houston study, -10°C to -40°C was used as the mixed phase zone. They found a strong correlation between the ice mass in the -10°C to -40°C region and the cloud-to-ground (CG) lightning. For the LVIF temperature profile, 0°C to -10°C was considered too warm based on KMLB's near tropical climate, consequently, -10°C to -40°C was chosen.

E. LIMITATIONS/GOALS

The LVIF technique is a new approach to correlate ice content and radar reflectivity to lightning potential. The LVIF technique builds upon the success of several previous studies. Gauthier et al. (2006) and Carey and Rutledge (2000) provided the foundation for the Z-M relationship, specifically in calculating ice mass. D'Arcangelo's (2000) application of the layered approach using VIL was the motivation for a layered frozen content approach. These previous studies provided a solid background for method and equations, as well as an insight to potential pitfalls. From this background, there are two known limitations at the onset of this study: 1. imperfections in the LVIF equation; 2. using a nonpolarized radar. These constraints are inherent to Z-M studies and have impacted previous studies in various ways.

Both Gauthier et al. (2006) and Carey and Rutledge (2000) concede that there is no perfect Z-M relationship. Carey and Rutledge (2000) used (2) out of necessity after observing that there was no "suitable" Z-M relationship in literature for deep tropical convection. However, discrepancies in the equation did not discernibly impact the success of either study. Carey and Rutledge (2000) concluded that CG lightning flash rate is well correlated to graupel mass. Gauthier et al. (2006) statistically analyzed a large data set to establish a near linear relationship between flash density and ice mass.

The Gauthier et al. (2006) study was also limited by a nonpolarized radar platform, but was still able to strongly correlate precipitation ice mass and CG lightning. However, Gauthier et al. (2006) experienced setbacks with their data set. Anomalies in the data were observed and despite the semi-linear relationship, they were forced to conclude that although the correlation between ice mass and CG lightning is strong, it is also “casual.”

Ultimately, there are three main goals for this study: 1. calculate LVIF; 2. analyze LVIF relationship to lightning occurrence; 3. assess lightning forecast potential. Calculating LVIF is a seven-step process described in Chapter II. Determining the relationship to lightning is the analysis of the results discussed in Chapter IV. The goals of this study are designed to build upon the work of previous research and to advance lightning forecasting.

THIS PAGE INTENTIONALLY LEFT BLANK

II. DATA

A. STORM DATABASE

In order to confidently match lightning strikes with their convective cell source, this study focused on analyzing isolated, single-cell thunderstorm events, also known as “pulse” storms. The 45 WS provided a spreadsheet of approximately 500 pulse storms from summer months (May-September) over a five-year period (2000, 2002-2005). The exact criterion used to select these pulse storms is unknown since the database was not compiled specifically for this study. However, all the events provided produced lightning and fulfilled the isolated single-cell constraint. The database recorded the following for each event: date, timeframe, location, and number of flashes.

In the spreadsheet provided by the 45 WS, each storm location was given with two latitude and longitude coordinates labeled southwest and northeast. The two coordinates, when graphed, formed a region around the storm, hereafter referred to as the storm box. The number of flashes is not explicitly defined, but is assumed to include the number of cloud-ground (CG), cloud-to-cloud (CC), and in-cloud (IC) strikes. This assumption is based on discrepancies between the number of strikes recorded by Air Force Combat Climatology Center (AFCCC) and number of flashes in the database. The Excel spreadsheet file also included some obscure/extraneous information that contained a graph axis labeled “LDAR Flashes.” The lightning detection and ranging (LDAR) system records all types of lightning. This brief reference among the rest of the dataset supports the assumption that the number of flashes also denotes all types of lightning.

Due to time constraints, not all the storms in this database could be analyzed, and the field was reduced first by choosing only the most recent years (2004 and 2005). Many of the dates had multiple storms at overlapping times. For simplicity, the dates that had only one storm per day were selected as a starting point. A total of six days from 2004 and 2005 met the two requirements; however, two were discarded due to their close proximity to the radar. Therefore, four cases were chosen for this study: 2 June 2004, 26 June 2004, 6 June 2005, and 15 June 2005.

B. RADAR

KMLB operates a Next Generation Weather Radar (NEXRAD) Weather Surveillance Radar-1988 Doppler (WSR-88D), which is a 10-cm (S-Band) Doppler radar (Roeder et al. 2005). The WSR-88D is the standard radar platform operated by the National Weather Service in 155 locations nationwide. The WSR-88D scans at 14 elevation angles (0.5°, 1.5°, 2.4°, 3.3°, 4.3°, 5.2°, 6.2°, 7.5°, 8.7°, 10.0°, 12.0°, 14.0°, 16.7°, and 19.5°) and takes five to six minutes to complete a full volume scan.

Level II radar data for KMLB was obtained through the National Climate Data Center (NCDC) website which provides free access to archived radar data. Radar data from NCDC came in a compressed tape archive (TAR) file that was uncompressed and opened using a radar reader program.

C. LIGHTNING

AFCCC provided lightning data for May through September 2004 and 2005. AFCCC lightning data is supplied by the Vaisala Inc. which owns and operates the National Lightning Detection Network (NLDN). The NLDN has been active since 1989 (Huffines and Orville 1999), but only records CG strikes. Lightning data included the location, date, time, polarity, strength, strokes, and number of detectors for each strike. The data came as a Comma Separated Values (CSV) file which stored every lightning strike for the requested time frame. The CSV file contained over two million lines of data and therefore required extensive sorting prior to use.

D. SOUNDING DATA

Sounding data from CCAFS (Station Id: 74794) was obtained through the University of Wyoming Department of Atmospheric Science's webpage which archives worldwide soundings. During the sample period, CCAFS conducted soundings several times a day at 0Z, 9Z, 15Z, or 21Z; usually at least three of the four times were available per day. The sounding closest to the time of each event is assumed to be representative of the atmosphere for the storm. Since all the storms are afternoon/evening events, the 15Z or 21Z sounding is used in all cases.

E. CHOSEN EVENTS

Coincidentally, all the events occurred in June and within the same general area (Figure 2). However, the strength, duration, and number of strikes varied considerably between storms.

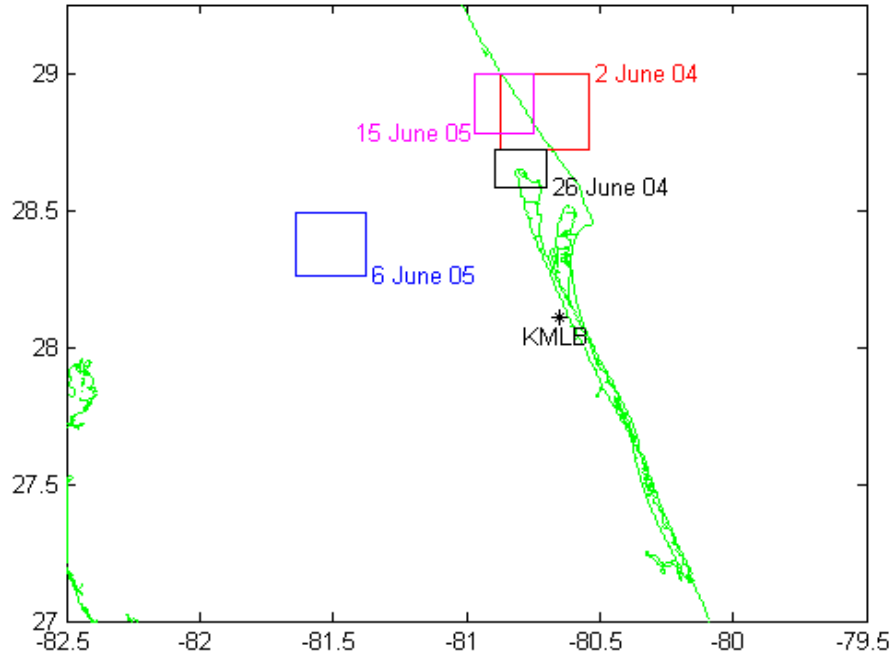


Figure 2. Locations of all storm boxes relative to one another and to the radar.

1. 2 June 2004

The 2 June 2004 event occurred from 18:57:17Z to 19:36:01Z (according to 45 WS dataset). It is assumed that the timeframe provided is the start and stop time for all lightning. During this time, the storm was 76 km north of KMLB over the Atlantic Ocean and moving eastward. There were a total of six CG strikes associated with this storm; the first of which occurred at 19:01:28Z and the last at 19:09:56Z. The 45 WS dataset recorded 23 flashes for this event. The extra 17 flashes are assumed to be lightning other than CG and the start time is unknown. As previously mentioned, the LVIF calculation uses a section of the storm between -10°C and -40°C . According to the Cape Canaveral 15Z sounding for this day, the temperature profile reached -10°C at

approximately 6200 m and -40°C at 10500 m. This storm could be identified on radar between scan angles 0.5° and 16.7° . Based on the distance from the radar this would be between 660 m and 22800 m.

2. 26 June 2004

The smallest and weakest of the four storms, the 26 June 2004 storm occurred from 16:31:50Z to 17:16:26Z. Located 61 km north of KMLB, there were four CG strikes and 16 flashes recorded in the dataset. The first CG strike occurred at 16:36:01Z. Using the 15Z sounding the LVIF range, -10°C to -40°C , was from 6200 m to 10500 m. This storm proved to be the most difficult to find on the radar with a limited vertical extent. This storm could be identified on radar between scan angles 0.5° and 8.7° . Based on the distance from the radar this would be between 530 m and 9300 m. This means that the radar could not see up to the -40°C level. Therefore, the -35°C to -40°C layer was omitted from the total LVIF. According to the CCAFS sounding, at 9300m the temperature was approximately -33°C . The -30°C to -35°C layer was still used since there is some error in the height calculation and most of the layer could be seen by the radar.

3. 6 June 2005

This is the shortest lived storm only lasting 25 minutes from 21:04:13Z to 21:29:13Z. The 6 June 2005 event was 89 km to the northwest making it the farthest from the radar. This large storm propagated south-southwest and produced only one CG strike, despite having a maximum reflectivity of 50 dBZ. The CG strike occurred at 21:16:39Z. The dataset logged 14 flashes associated with this storm. The 21Z sounding had some missing data after -31°C which prevented the entire sounding to be read by MATLAB. Therefore, this storm was only analyzed from -10°C to -35°C . For this modified LVIF range, the 21Z sounding showed the LVIF range from 6500 m to 10000 m. This storm could be identified on radar between scan angles 0.5° and 7.5° . Based on the distance from the radar this would be between 770 m and 11700 m.

4. 15 June 2005

This was the longest storm, lasting over an hour from 17:28:48Z to 18:55:30Z. Located in the same area as the 2 June 2004 storm, the 15 June 2005 event was 74 km north of KMLB. As the longest-lived storm, this event had the most CG strikes, with 41 strikes recorded by AFCCC and 200 flashes in the dataset. The first CG strike occurred at 17:33:54Z. The 15Z sounding for the day, showed the -10°C to -40°C layer from 6700 m to 10800 m. This storm could be identified on radar between scan angles 0.5° and 10.0°. Based on the distance from the radar this would be between 640 m and 13000 m.

THIS PAGE INTENTIONALLY LEFT BLANK

III. METHODS

A. RADAR

The first step was to manipulate the raw Level II radar data into a useable format using a reader program. The next steps in calculating the LVIF required the radar to be plotted in a Cartesian coordinate system. There were no reader programs available or provided that could accomplish the coordinate system transformation. Therefore, Professor Wendell Nuss, Naval Postgraduate School, developed a FORTRAN reader program specifically for this data set. The reader program translated the Level II radar data into a useable grid centered at the Melbourne radar and reaching a 150 km radius. The grid covered a 300 km by 300 km area and had a resolution of 250 m. The purpose of the grid was to transform the reflectivity and height into a Cartesian coordinate system.

The radar data included two datasets: reflectivity and height. For every storm, there is reflectivity data for each elevation angle (14 for each full volume scan) and for each complete scan.

1. Reflectivity

Using Cartesian coordinates simplified the programming to overlay lightning and storm locations. Using MATLAB, the grid that was developed in the reader program was recreated in a visual format. The reflectivity was read in and plotted on a grid of the same dimensions (Figure 3). The plot provided a visual aid to determine the location, intensity, vertical extent, and development. Each storm was plotted for approximately 30 minutes prior to the first CG strike which equates to six full volume scans.

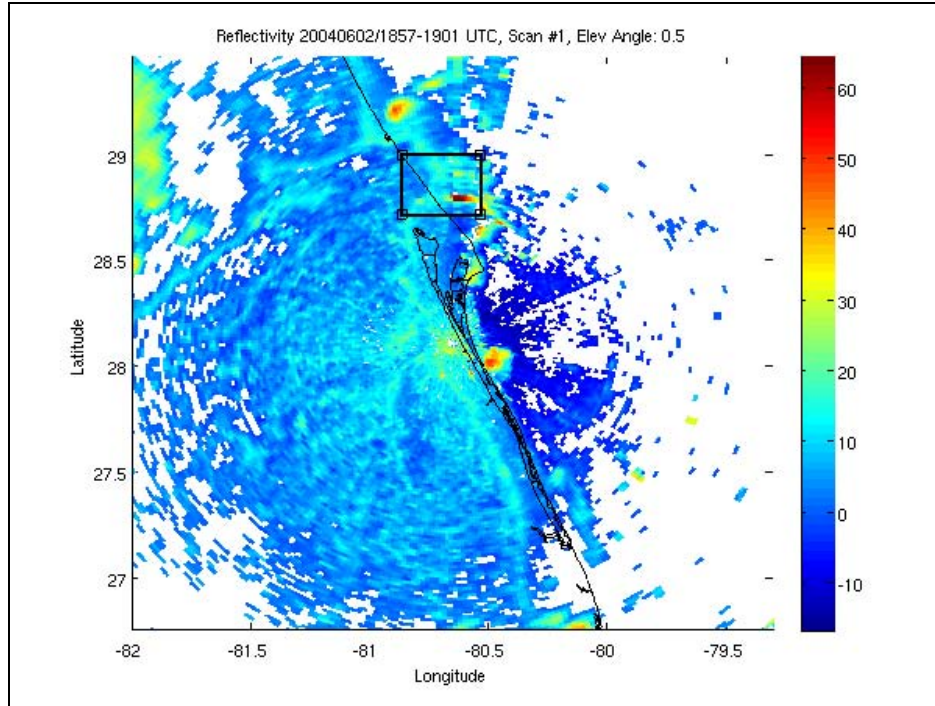


Figure 3. Sample of the reflectivity grid taken from 2 June 2004, elevation angle 0.5°. The boxed area indicates the storm location.

2. Height

The radar data set included a height variable for each grid point. However, the official height was not used because the elevation angles were not constant for the entire scan. Instead, while the radar completed a scan at a specific elevation angle, there appeared to be a “wobble” as the radar changed from one elevation angle to the next. This “wobble” created a discontinuity in the height at each grid point so that adjacent grid points had the potential to be 100-300 meters difference in height (Figure 4). Even at the same elevation angle the discontinuities occurred at a different location for each scan.

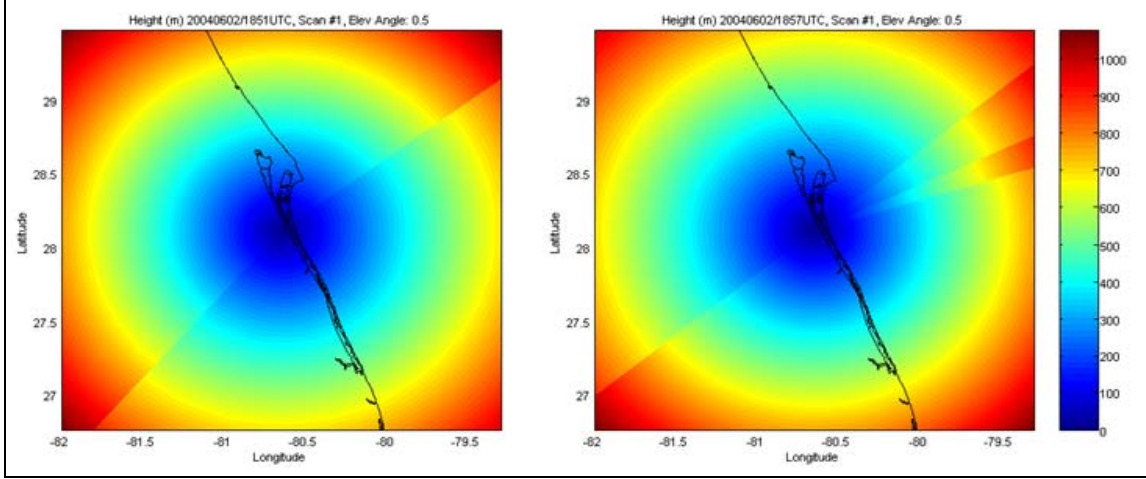


Figure 4. Discrepancies with height between two scans at the same elevation angle (0.5°).

The height parameter is required in later steps to chart the LVIF values in the vertical, so the standard elevation angles (i.e., 0.5°, 1.5°, 2.4°, etc.) were used to calculate the height at every grid point for each scan. Calculating the height in this way created 14 reusable scan heights instead of providing different height profiles for every scan, while at the same time simplifying the MATLAB programming. In the operational environment, the difference in elevation would not be available to the forecaster, making this simplification a reasonable assumption.

Height is calculated in a two-step method for every grid point:

1. Calculate the great circle distance (Meridian World Data) from the radar to the grid point,

$$distance_{km} = r_{earth} \times \arccos \left(\sin\left(\frac{KMLB_lat}{57.2958}\right) \sin\left(\frac{point_lat}{57.2958}\right) + \cos\left(\frac{KMLB_lat}{57.2958}\right) \cos\left(\frac{point_lat}{57.2958}\right) \cos\left(\frac{point_lon - KMLB_lon}{57.2958}\right) \right) \quad (5)$$

2. Calculate the tangent of the elevation angle and multiply by the distance,

$$height_m = \tan(elevation_{radians}) \times distance_{km} \times 1000 \quad (6)$$

This calculation assumes a straight line beam path and does not account for the height of the antenna or refraction. Using equation (6), the height of each elevation angle was plotted for distances up to 100 km from the radar (Figure 5).

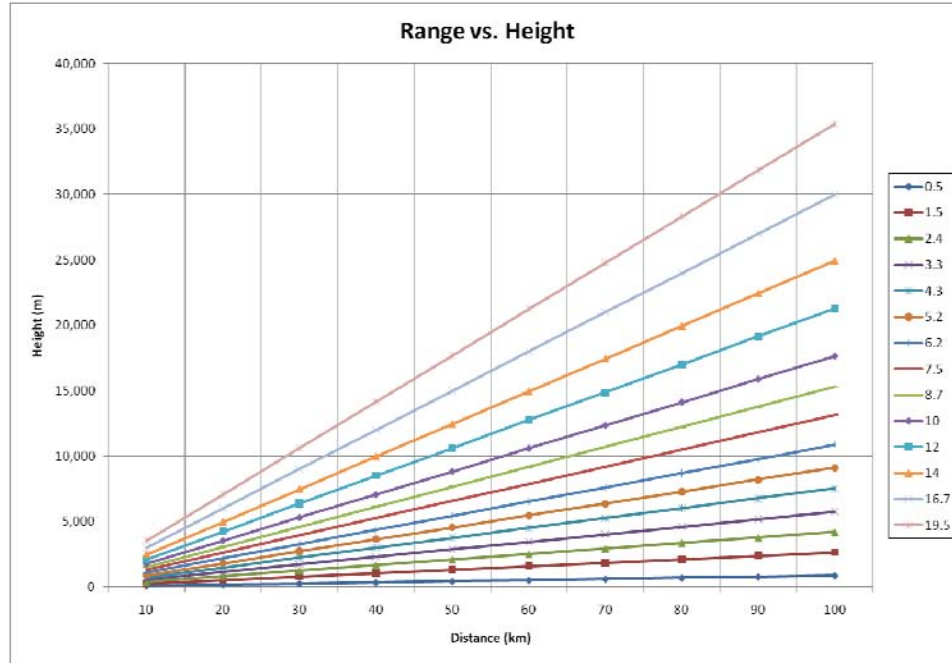


Figure 5. Distance from the radar to the storm versus height.

B. LIGHTNING

Lightning data from AFCCC was provided in a large CSV file listed by strike date and time. To isolate the data for the four events, the strikes were sorted and plotted in a four-step process using MATLAB. First, the CSV file was divided into two CSV files, one for 2004 and one for 2005. Then, each year was sorted for the desired dates and CSV files were created for each full day. The third step decoded the daily CSV file, saved variables into a MAT file, and generated a plot of the lightning strikes for the entire day. (This step was critical to making the variables (i.e., date, time, location) more accessible.) Finally, lightning for each storm was isolated using the storm timeframe and storm box (Figure 2). Strikes that occurred during the same time and within the storm box were counted for the storm; any strikes outside of the storm box were not counted.

For each full volume radar scan, lightning strikes were overlaid on the radar grid. Although each full volume scan takes five to six minutes to complete, the time of the scan was treated as if it occurred instantaneously. Lightning occurring during a scan was considered to be a product of that five minute scan so that multiple strikes could be on each scan. The original motivation for the lightning data was to match it with the radar

image that coincided with the strikes. Potentially, this would help identify a threshold for storm structure at the time the lightning occurred. It also proved inconclusive regarding cell structure and lightning production. This might prove useful if complete data regarding cell structure and evolution could be obtained. Furthermore, until more fruitful data surfaces, it may not be useful for watches and warnings. However, since watches and warnings must be issued prior to lightning onset, the structure and build up of the storm was more important and the overlaid lightning-radar images were abandoned.

C. LVIF CALCULATIONS

There are two variables evaluated in the LVIF calculation: reflectivity and the thickness of the layer. The layer thickness is fairly consistent for each storm and between each layer so it does not strongly influence the LVIF value. Although it is a nonlinear relationship, there is a positive correlation causing the larger reflectivity returns to produce larger LVIF values. The total LVIF calculation from the radar is a seven-step process. The first five steps develop a vertical plot of reflectivity versus height over a designated location. The last two steps calculate the ice mass and the total LVIF for the -10°C to -40°C layer.

1. Vertical Plot

Each of the following steps was completed for all four cases. The first step in the LVIF calculation was to manipulate the sounding data. The CCAFS sounding data was ingested into MATLAB and interpolated to extract the height of the specific temperature levels. This step is required since the reflectivity at specific temperature heights is needed and do not coincide with the height of the scans. For the four storms, the -10°C isotherm on average was at 6000 m. The -40°C isotherm height was approximately 10500 m. Calculating the height of each elevation angle using the location of the storm is the second step. Next, the first angle that is at or above the -10°C height ($\sim 6000\text{m}$) is determined. This elevation angle will be referred to as the start elevation. For example, in the 2 June 2004 case, 4.3° crossed the storm at 5714 m, under the -10°C isotherm. The 5.2° crossed at 6917 m, above the -10°C isotherm. Since the 5.2° scan fell within the -10°C to -40°C range (6000 m to 10500 m), then 5.2° is the start elevation. The start

elevation is dependent on the distance from the radar, so it is different for each storm. Therefore, the start elevation for 2 June 2004 is 5.2° ; 26 June 2004 the 6.2° scan; 6 June 2005, the 4.3° scan; and 15 June 2005, the 5.2° scan.

Since large reflectivity returns produce large LVIF values, the region of maximum reflectivity is the most important. However, the maximum reflectivity at each elevation angle does not occur over the same location (Figure 6a and 6b). Using the 2 June 2004 case as an example, in the storm box, the maximum at 5.2° (Figure 6a) is between -80.65°W and -80.67°W . The maximum at 8.7° (Figure 6b) is to the west between -80.69°W and -80.70°W . Therefore a maximum at one elevation angle is not at the same location as the elevation angle above or below it.

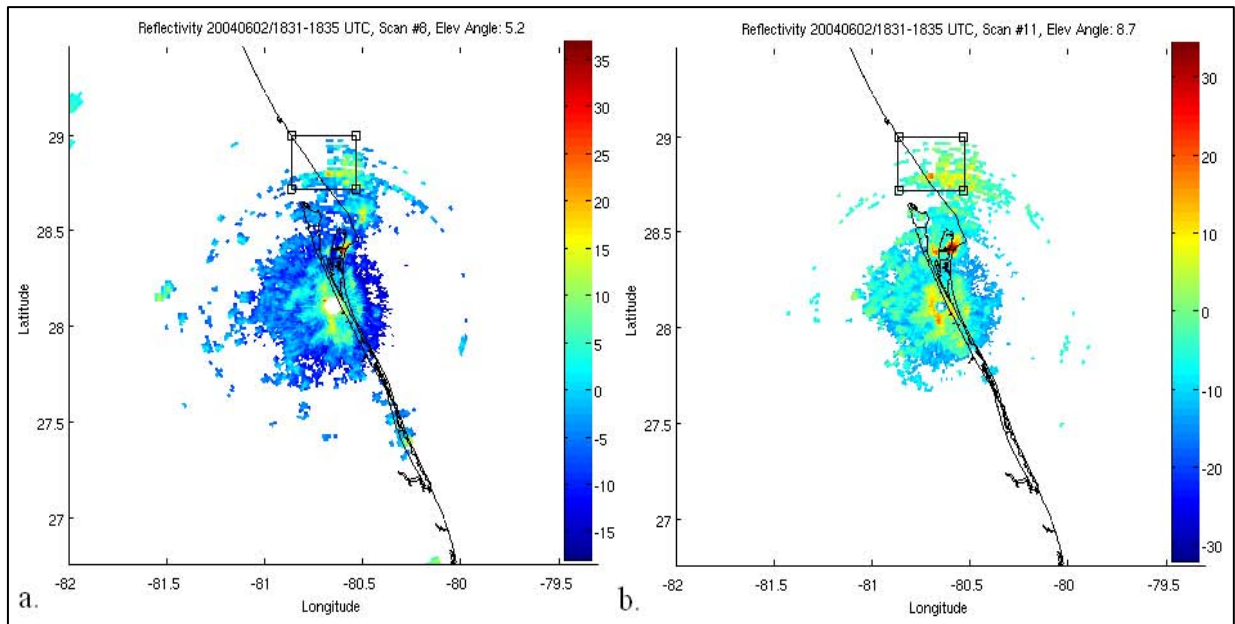


Figure 6. Example from 2 June 2004: a. Elevation Angle 5.2° ; b. Elevation Angle 8.7° .

The MATLAB program required specific coordinates to extract the reflectivity in the column for the vertical plot. The coordinates were taken from the start elevation scan. Selecting these coordinates is the fourth step in calculating LVIF. The location of the maximum reflectivity relative to the boxed area is recorded for each full volume scan. This was accomplished using the MATLAB data cursor tool.

The locations of maximum reflectivity at the start elevation are recorded for all scans prior to the first CG strike. The Z values from all the elevation angles were extracted from the radar grid at the latitude and longitude chosen by the MATLAB data cursor tool. Since the elevation angles only hit the storm in distinct points, a spline was used to create a possible reflectivity curve (Figure 7). Creating the spline is step five.

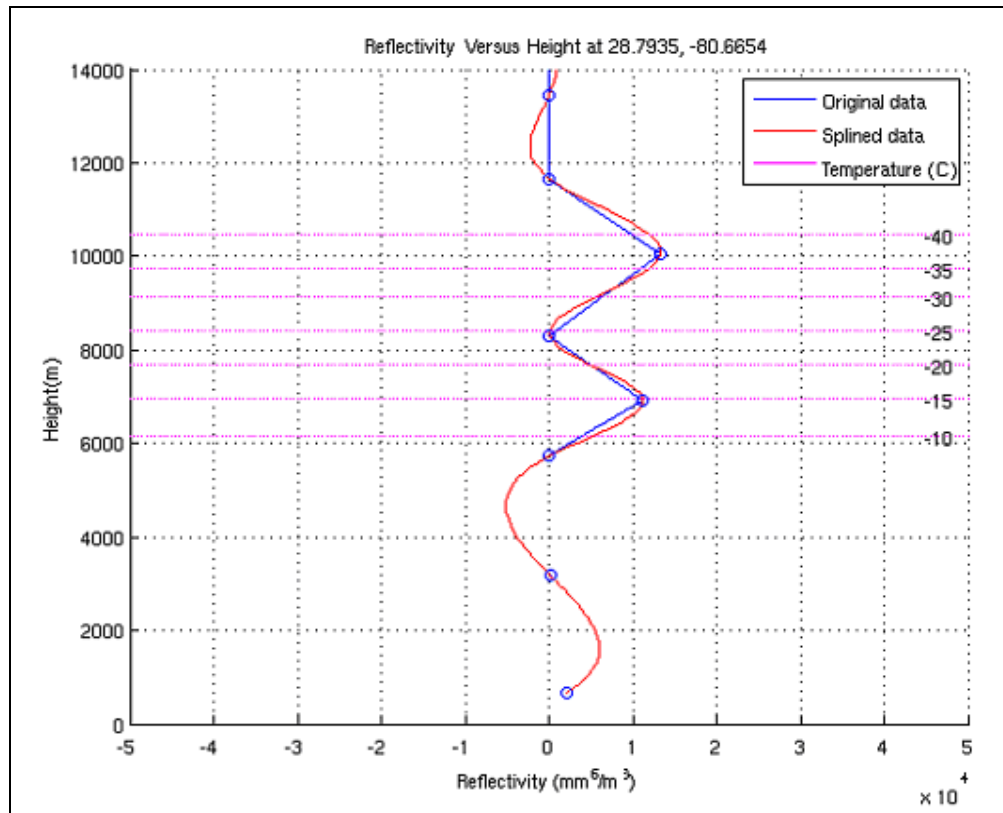


Figure 7. Sample Reflectivity with Height Spline plot from 2 June 2004.

As the storms moved over the 30 minute timeframe, different latitudes/longitudes were sampled, but the sample was always the maximum reflectivity and at the start elevation angle. The -10°C to -40°C layer is only a thin slice of the total storm on the radar and encompasses three or four elevation angle scans. Identifying a reflectivity, at a specific point, in a specific temperature range, depends greatly on how well the storm is sampled and splined by the MATLAB program.

2. Ice Mass

The vertical plot (Figure 7) is not required to perform the LVIF calculation, since the splined data is stored in MATLAB variables, but it provides a visual check of the data. In the sixth step, the splined data was used to calculate the LVIF for each 5°C level (-10°C, -15°C, -20°C, -25°C, -30°C, -35°C, -40°C). Since the splined curve is simply the computer's best-fit curve and interpolation of missing data from a noncontinuous dataset, the spline included some negative reflectivity values. The negative reflectivities caused two problems: 1. they created imaginary LVIF values and 2. Negative values do not exist in nature. For the purpose of the LVIF calculations, all negative reflectivities were treated as zeros. Finally, the LVIF values from each 5°C layer were summed up to arrive at the total LVIF. Each temperature layer was analyzed individually to see if one layer was more important than another. D'Arcangelo's (2000) thesis identified two layers -10°C to -15°C that were more important in LVIL so there may be a region of the atmosphere more important to LVIF.

IV. RESULTS

A. LVIF RESULTS

The LVIF results of each storm were plotted over time in two different ways. First, the total LVIF was plotted (Figure 8a through 11a) and then the LVIF for each layer was plotted (Figure 8b through 11b). The total LVIF indicates the overall trend of the frozen content before the first strike. The subdivided LVIF is used to identify the most important layers. The most important layer is defined as the layer that had the largest ice content during a specific volume scan. As described in the methods section, where the reflectivity spline produced a negative value, these layers were treated as zeros. Therefore, in the subdivided plots, any missing values are these zeroed layers. This occurred in plots 9b, 10b, and 11b. The trends of the subdivided LVIF follow the trends from the total LVIF. In general, time periods with a maximum total LVIF have large LVIF values at each layer.

For both the total and subdivided plots, LVIFs were calculated for a total of 35 minutes or seven scans; every five minutes for 30 minutes prior to the first CG strike and first full scan after the first strike. The label 30-25 means between 30 and 25 minutes before the first CG strike. Each full volume scan lasts five to six minutes but the reflectivity and lightning are treated as being instantaneous. The 5-0 label indicates that the first CG strike occurred during that volume scan. The 0-+5 label means the first full volume scan after the first strike.

1. 2 June 2004

Over the 30 minutes prior to the first CG strike, the 2 June 2004 storm had increasing total LVIF values (Figure 8a). At the onset of CG lightning, the total LVIF sharply decreased and continued to decrease after the first strike. The highest total LVIF for this event, 3.4486 g/m^2 , occurred during the 10-five minute scans. The layers with the greatest ice content for this storm were the -10°C to -15°C layer and the -35°C to -40°C layer (Figure 8b). The -10°C to -15°C layer had the largest ice content in four of the seven scans, at 30-25, 25-20, 15-10, and five-zero minutes. The -35°C to -40°C layer

had the largest ice content in two of the seven scans, at 20-15 and 10-five minutes. The final scan, zero-plus five, had the largest ice content in the -25°C to -30°C layer. In the final scan, all the layers had almost equal ice content. The layers that had the least ice content varied from scan to scan but were most commonly between -15°C and -35°C.

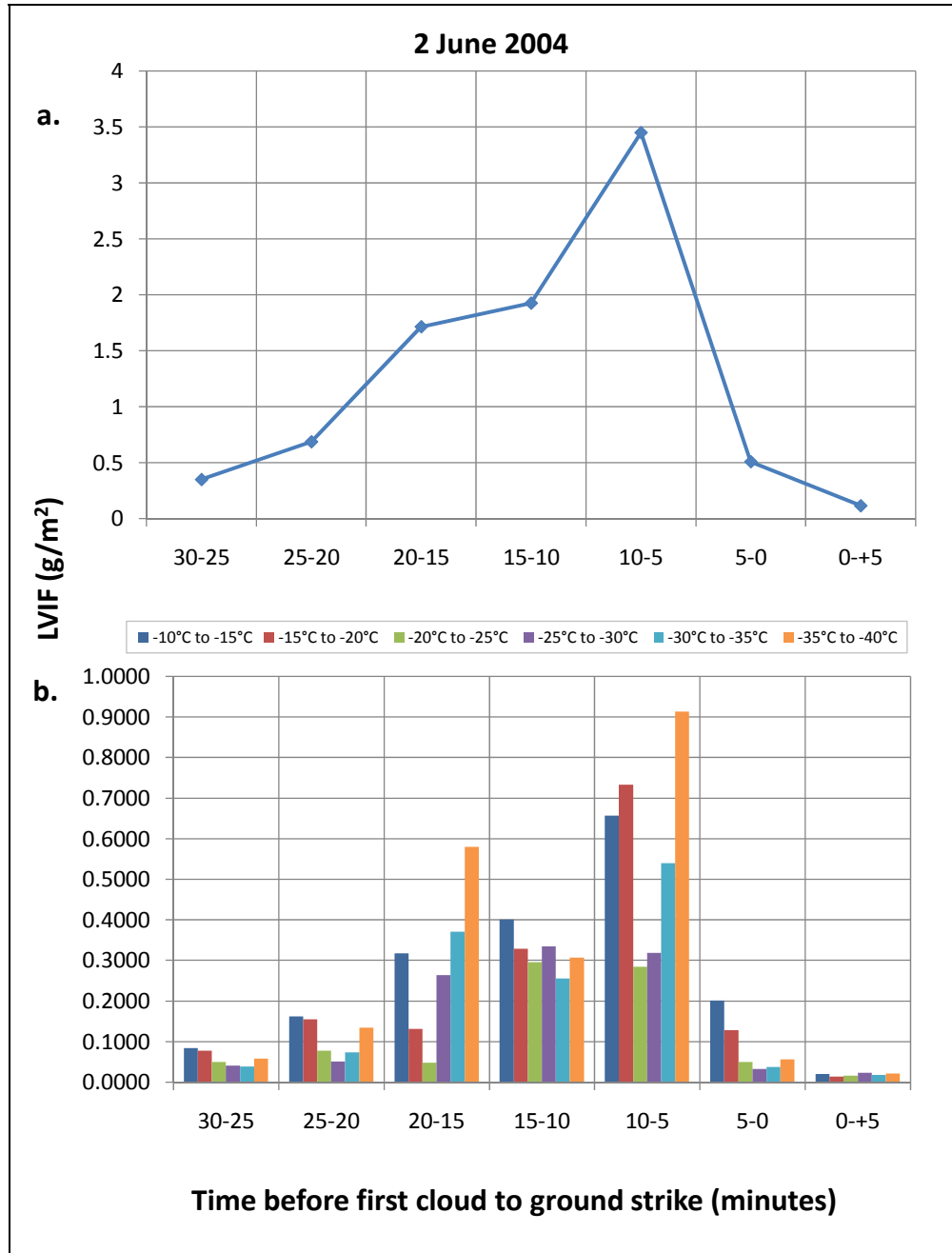


Figure 8. a. Total LVIF for 2 June 2004. b. LVIF of each thermal layer for 2 June 2004.

2. 26 June 2004

The 26 June 2004 storm was the weakest storm and produced the smallest LVIF values. Throughout the 30 minutes prior to the first strike, the total LVIF fluctuated with a maximum of 0.0983 g/m^2 (Figure 9a). This maximum in ice content was almost five times larger than the next highest LVIF of 0.0205 g/m^2 . The peak value for the 26 June 2004 storm occurred between 20 and 15 minutes before the first strike. When subdivided by layer (Figure 9b), during the 20-15 minute scan, ice content was at a maximum in every layer. For this event, the -10°C to -15°C layer contributed the most to the total LVIF in five of the seven scans. The -25°C to -30°C layer contributed the most to the total LVIF in two scans and was the most contributing layer during the 20-15 minute scan.

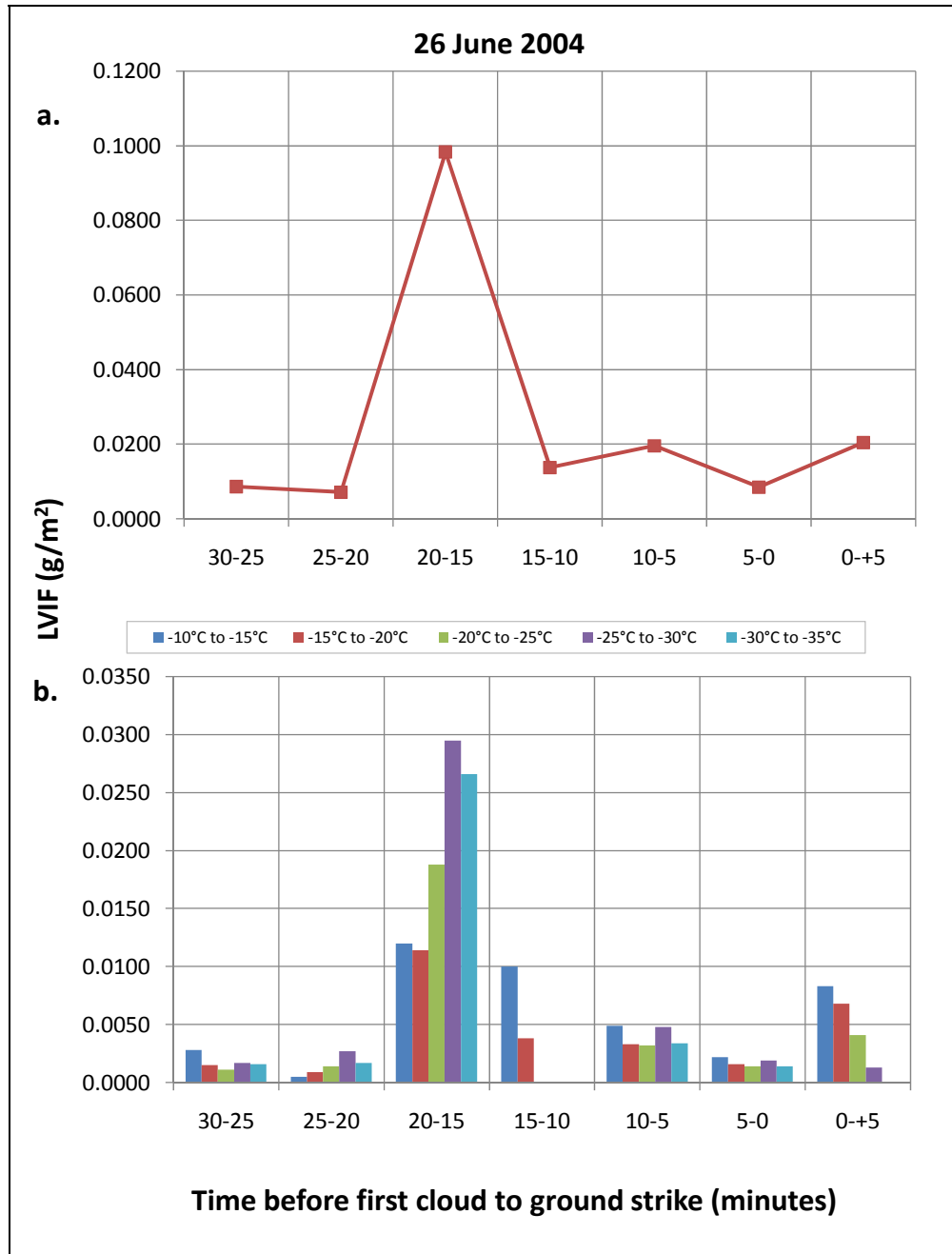


Figure 9. a. Total LVIF for 26 June 2004. b. LVIF of each thermal layer for 26 June 2004.

3. 6 June 2005

The 6 June 2005 storm also had some fluctuation in total LVIF, but displayed an overall decreasing trend (Figure 10a). The maximum on 6 June 2005 was 1.5636 g/m² and occurred 25-20 minutes before the first strike. There was also a secondary peak at

15-10 minutes where the LVIF was 0.8040 g/m^2 . For this event, the -30°C to -35°C layer contributed the most to the total LVIF in five of the seven scans, including the 25-20 minute scan (Figure 10b).

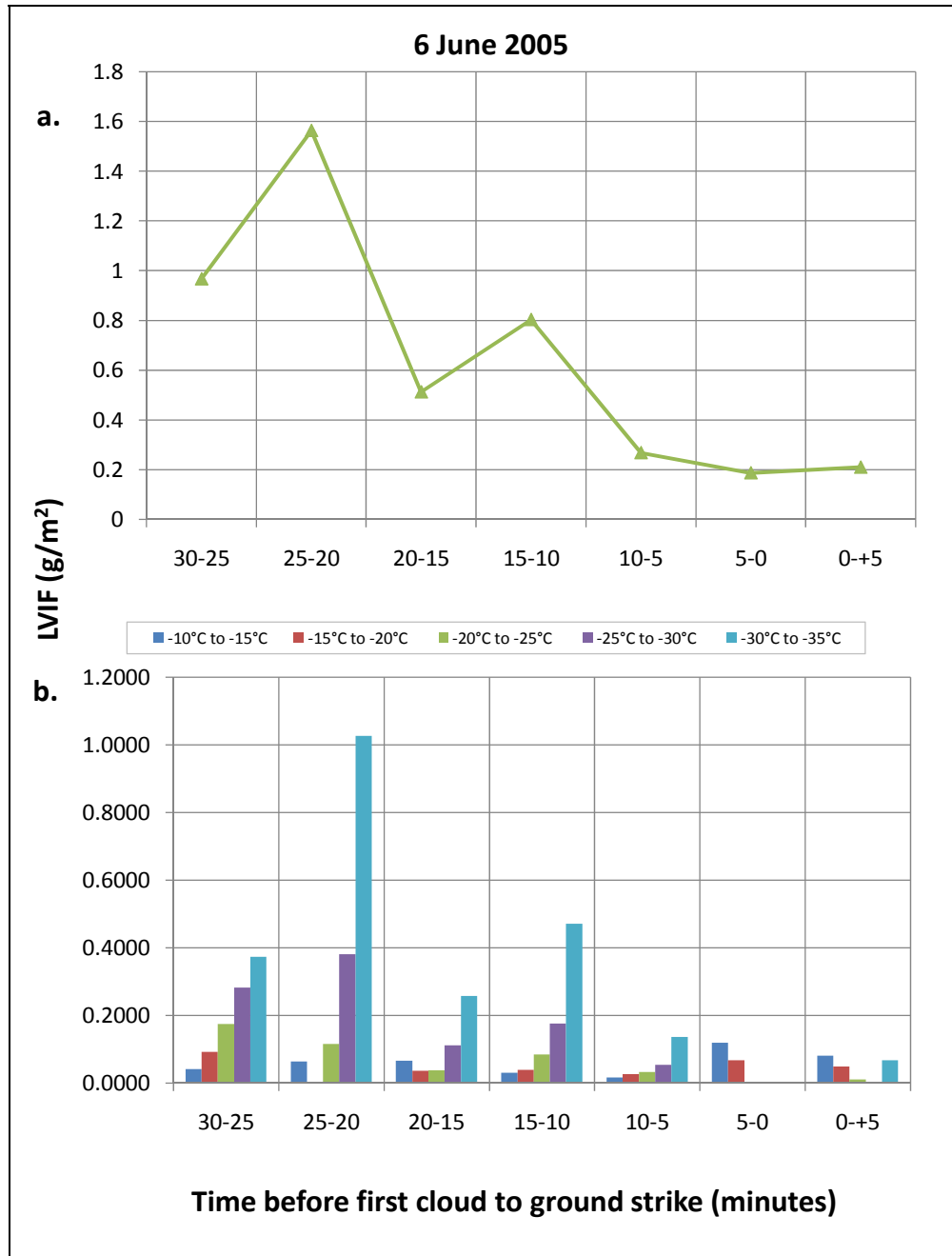


Figure 10. a. Total LVIF for 6 June 2005. b. LVIF of each thermal layer for 6 June 2005.

4. 15 June 2005

Finally, the 15 June 2005 storm had a sharp increase in ice mass at the time of the first strike and continued to have increasing LVIF values after the first strike (Figure 11a). Prior to the first strike, the maximum LVIF was 5.3171 g/m^2 ; after the first strike, the LVIF reached 6.9534 g/m^2 . This storm was the largest of the four with 41 CG strikes. The layer that contributed the most to the total LVIF was the -35°C to -40°C layer (Figure 11b). The -35°C to -40°C layer had the maximum ice content in three of seven scans. However, the maximum ice content in the other four scans was in four different layers: the -10°C to -15°C layer, the -20°C to -25°C layer, the -25°C to -30°C layer, and the -30°C to -35°C layer.

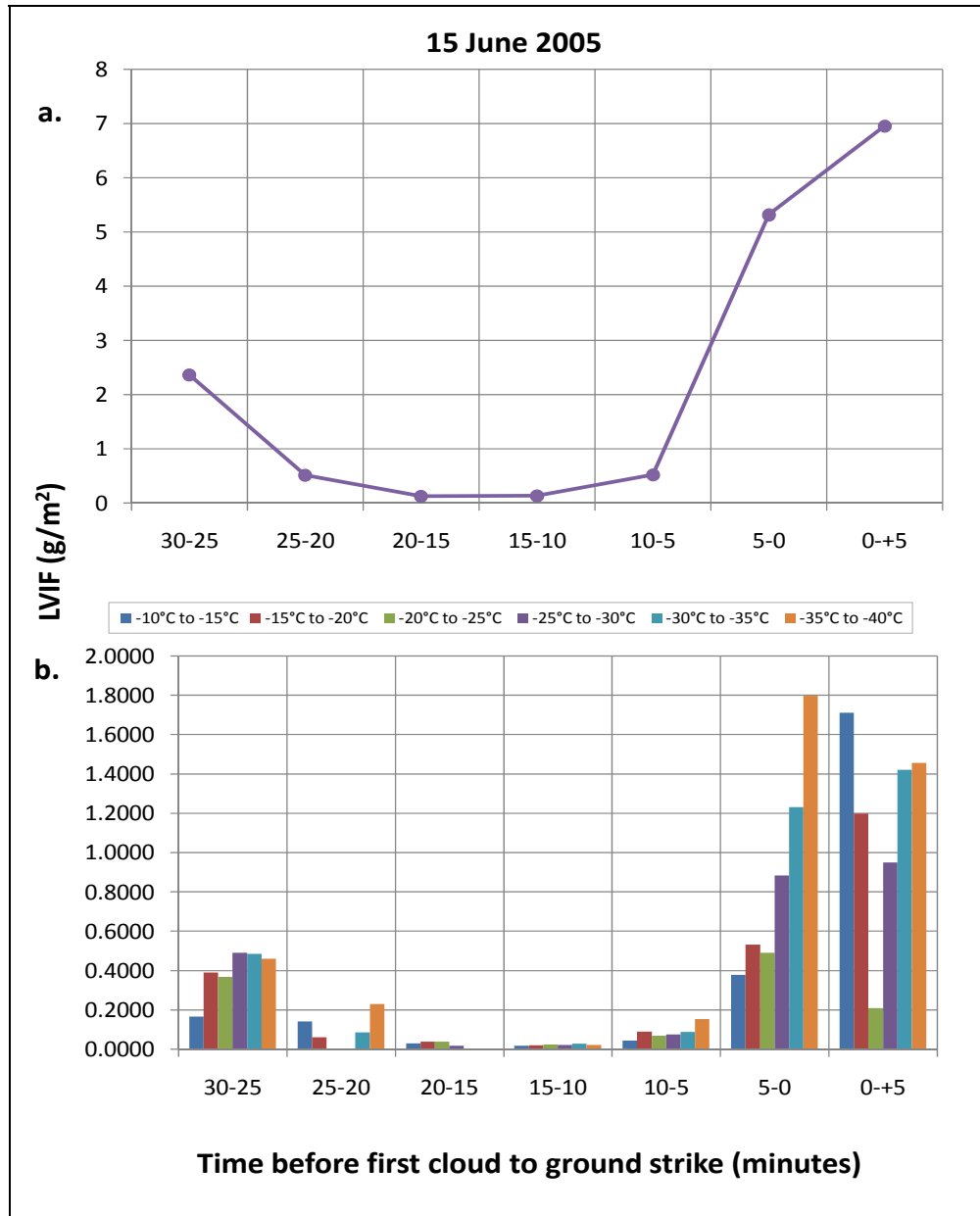


Figure 11. a. Total LVIF for 15 June 2005. b. LVIF of each thermal layer for 15 June 2005.

5. Comparison of all Storms

The magnitude of the LVIF values varied greatly from storm to storm. The highest value observed was 6.9534 g/m² on 15 June 2005. The lowest observed value was 0.0072 g/m² on 26 June 2004. Overall, there were a broad range of values from each storm (Figure 12a). LVIF does not correlate well to storm strength. For example, the

6 June 2005 storm only produced one CG strike (14 flashes), but maintained LVIF values greater than the 26 June 2004 storm, which had four strikes (16 flashes). Furthermore, the 15 June 2005 event had LVIFs significantly greater than the other three storms and this storm also had the largest number of strikes, 41 (200 flashes). However, the LVIF values from 25 minutes to five minutes prior were not significantly greater than the other storms, providing no indication that 15 June 2005 would be a big event.

In addition to variations in magnitude, the timing of maximums was also inconsistent. Maximum LVIF occurred at a different time for each storm. This is not surprisingly since every thunderstorm develops at a different rate. However, there is no trend of growing or decaying ice mass prior to lightning onset. There is also no layer that was consistently most important. The -10°C to -15°C layer had the greatest ice content for the 2 June 2004 storm and the 26 June 2004 storm. The -30°C to -35°C layer had the greatest ice content for the 6 June 2005 storm and the -35°C to -40°C was contributed the most to the 15 June 2005 storm.

Ice content and reflectivity do not have a linear relationship. However, there is a positive relationship when using the LVIF equation; large reflectivity values produce large ice content results (Figure 12a and Figure 12b). For the 2 June 2004 event, the largest total LVIF occurred with reflectivity of 50 dBZ. For the 26 June 2004 storm, the reflectivity during the largest LVIF was 23 dBZ. The reflectivities for 6 June 2005 and 15 June 2005 were 45 dBZ and 55 dBZ, respectively. The three storms, 2 June 2004, 6 June 2005, and 15 June 2005, had maximum reflectivities that were close in value. Additionally these three storms had a similar range of values during the entire events. The 26 June 2004 event had reflectivities that were extremely low in comparison.

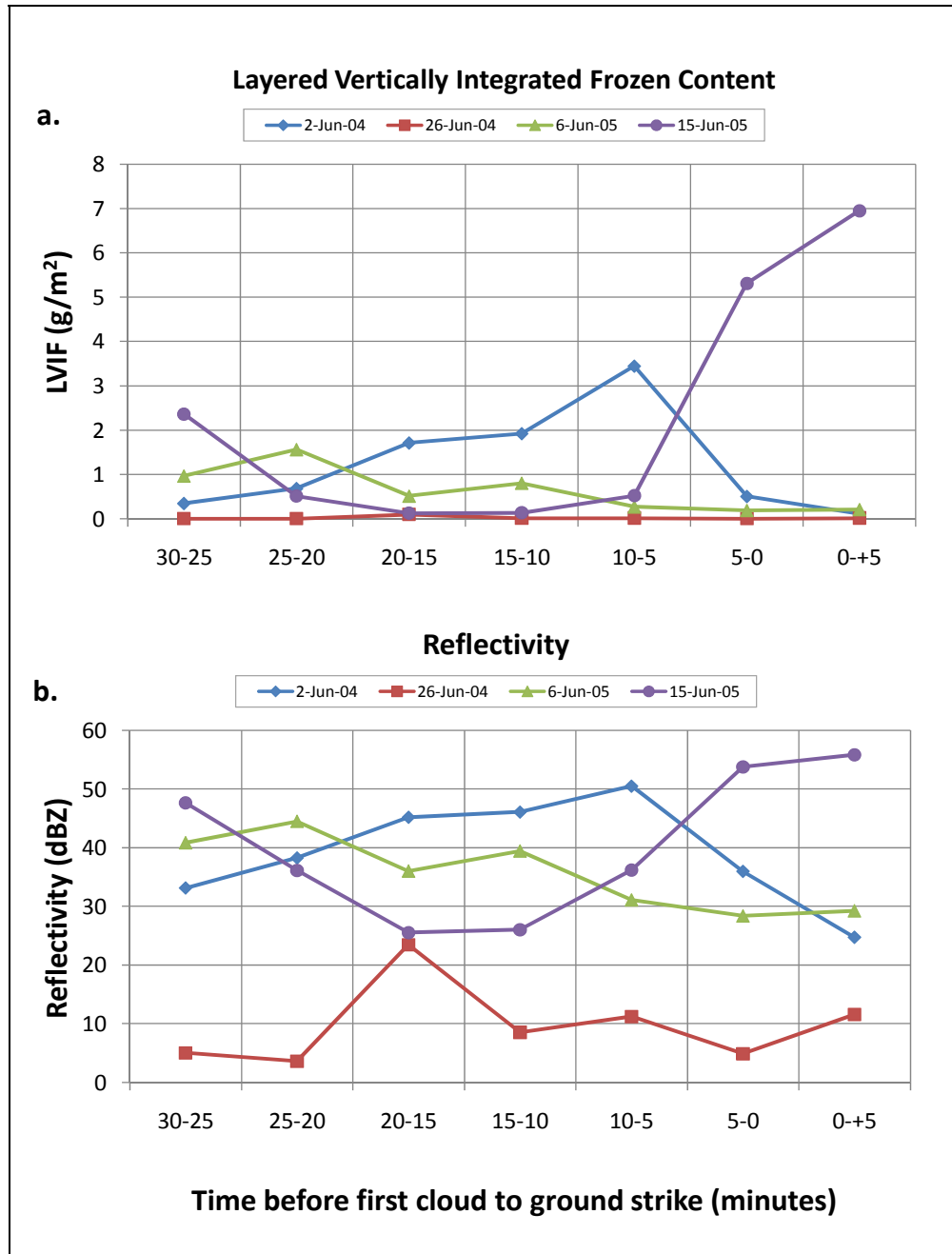


Figure 12. a. Total LVIF for all the storms. b. Reflectivity averages for all the storms

Dye and Willett's (2007) field work provides a possible explanation for this apparent anomaly. Dye and Willett (2007) studied anvils over Florida near CCAFS/KSC during June 2000 and June 2001. They observed two anvils with reflectivity 20-25 dBZ which maintained their electric field for many tens of minutes well downstream of the

convective core. Dye and Willett (2007) concede that although the two anvils did not produce lightning, the electric field was probably sufficient to trigger lightning for many tens of minutes. In the 26 June 2004 case, the reflectivity was much lower than that of the other three storms and had reflectivities similar to those in the Dye and Willett (2007) study. Therefore, based on Dye and Willett (2007), the lightning in this event may have been from an anvil cloud.

V. CONCLUSIONS AND RECOMMENDATIONS

The purpose of this study was to analyze lightning producing storms over Florida and relate that lightning potential to ice content using a Z-M relationship. The goals set forth at the beginning were to: 1. calculate LVIF; 2. analyze LVIF relationship to lightning occurrence; 3. assess lightning forecast potential. In the four storms that were analyzed, there was no apparent trend in LVIF, nor was there a layer that had the most impact. This section will discuss, first, how well the goals were met and, second, any conclusions that can be drawn from the results.

A. GOALS ACCOMPLISHED

1. Data Handling

Before the LVIF could be calculated, there were three areas of data preparation that were successfully completed: the radar reader program, sorting through the lightning data, and manipulating the sounding data for use in the spline. The radar reader program provided a visual representation of the storm and was robust enough to extract the reflectivity at specified locations. The lightning data was extensive and cumbersome. However, the needed information was successfully obtained for each storm to include, isolating the strikes with the storm box during the time of the storm and counting the total CG lightning strikes. Lastly, the sounding data was acquired and put into a format so it could be used in the LVIF calculation.

2. Calculate LVIF

Calculating LVIF was a seven-step process that encompassed the largest portion of the study. The steps were as follows: 1. interpolate sounding data to extract the height of the -10°C isotherm; 2. calculate the height of each elevation angle using the location of the storm; 3. determine the start elevation; 4. find the maximum reflectivity at the start elevation and select coordinates; 5. ingest coordinates into MATLAB program and create spline; 6. use spline to calculate LVIF at each layer; 7. and calculate the total LVIF by summing the LVIFs from each layer.

The LVIF for all four storms was calculated. All seven steps were completed for each storm. However, it is difficult to know the degree of accuracy in the LVIFs. Based on the results, the storms are listed in order of accuracy confidence: very confident in the accuracy of 2 June 2004 LVIF, somewhat confident with the accuracy of 6 June 2005 and 15 June 2005 LVIF, and not confident with the accuracy of the 26 June 2004 LVIF results.

The 2 June 2004 storm had strong, deep convection that could be seen by the radar up to 22800 m. For this storm, we can confidently state that the radar observed the entire storm. The 2 June 2004 spline sampled this storm well and the LVIF seemed to have a good correlation to the build up to lightning.

The 6 June 2005 storm was 89 km from the radar, which prevented the entire storm from being seen by the radar. Also the sounding data was missing above -35°C so a complete LVIF (up to -40°C) was not calculated. Therefore, this storm was given a lower confidence rating on LVIF accuracy.

The 15 June 2005 event was the most lightning producing storm with 41 CG strikes and became the largest of the four storms. However, in the 30 minutes prior to CG lightning, the storm was elusive on the radar until just before the first CG lightning. From this observation, we can conclude that the storm did not fully develop until about 10 minutes prior to the first CG strike.

Finally, the 26 June 2004 storm was extremely weak and was not picked up well on the radar. This storm is an anomaly since the extremely weak reflectivity still produced four CG lightning strikes. It is possible that this was actually an anvil cloud, but without further research, cannot make a definitive conclusion in this area.

3. LVIF Relationship to Lightning

Based on the low confidence in the LVIF calculations, a relationship to lightning could not be found. There appeared to be no discernible patterns in LVIF leading up to CG lightning. Also, there did not seem to be a layer that was the most important to the total LVIF. Previous research had made correlations between ice mass and about flash

rate (Carey and Rutledge 2000) and ice mass and flash density (Gauthier et al. 2006). This study was attempting to make definitive conclusions ice mass and lightning onset. This goal was not met.

4. Lightning Forecast Potential

Since a relationship could not be found between LVIF and lightning onset, the next goal of applying it for forecaster use was also unrealized. Ideally, had a trend been identified then the next step would have been to find a way to put this into operational use. Unfortunately, this goal was also unrealized.

THIS PAGE INTENTIONALLY LEFT BLANK

VI. DISCUSSION

A. SOURCES OF ERROR

The small sample size was a large contributing factor. However, even with so few storms, there are steps that could have been performed differently that may have positively altered the LVIF results.

1. Data

a. Lightning Data

As previously mentioned, little information was provided regarding the development of the storm dataset. Not knowing the origin of the dataset, led to two errors. One discrepancy, already observed, is that the number of flashes is greater than the number of strikes. In retrospect, lightning data should have also been obtained from the Global Hydrology Resource Center (GHRC) that archives LDAR data which records all flashes (not only CG strikes). LDAR is located at KSC, 47 km due north of KMLB. This puts the LDAR in the optimal range for the KMLB radar. A second option for lightning data is to obtain it from the 45 WS. Either approach would have resulted in a more robust lightning dataset.

The second problem with the dataset is with the storm time frame. The start and end of each event extend beyond the times of the CG lightning. In all the cases, the first CG strike occurs several minutes after the start of the storm and the storm persists for awhile after the last CG strike. Most likely, the storm timeframe given is the start and end of all types of lightning for that particular pulse storm. Since the LVIF was calculated 30 minutes prior to the first CG strike, an LVIF calculation prior to the first flashes (or start time) would have sampled a different time period.

b. Missing Data

Two data sets were unavailable: satellite imagery and storm observations. Satellite imagery would have been helpful in analyzing the synoptic situation. The differences in LVIF values and trends could be due to the different types of storms that

produced the lightning. Although they were all pulse storms, they did not all develop in the same manner or to the same intensity. In order to make appropriate comparisons, it would have been preferable to include storms developing from the same atmospheric phenomenon such as resulting from the sea breeze, for example. Observations of these storms were not available since they were not directly over any observing stations.

2. Calculations

The first assumption involved using the polarized radar equation with a conventional (non-polarized) radar dataset. It is difficult to estimate the percentage of error attributable to this assumption; however, it is a source of error. In comparison, LVIF produces values that are significantly smaller than LVIL values. This is to be expected since, mathematically, the LVIF calculation has units that are three orders of magnitude smaller than the LVIL. The results show little correlation between LVIF and the start of CG lightning. The shape of the LVIF plot would be no different if it had been calculated for LVIL because the main difference between the two is the coefficient. If Z_{ICE} could have been extracted then the plot might have appeared different.

The second error came from the simplified height calculation. The actual height calculation (7), taken from the National Weather Service, uses a refractive index (RI) of 1.21 and 6371 km as the radius of the earth:

$$height_m = [distance_{km} \times \sin(elevation_{radians}) + \frac{distance_{km}^2}{2(RI)(radius_{earth})}] \times 1000 \quad (7)$$

As a result, compared to the actual beam height, the height used is an under estimate in elevation angles less than 14° and an over estimate in elevation angles greater than 14° (Figure 13). The LVIF range, -10°C to -40°C, for the studied storms is most often between elevation angles 4.3° and 8.7°. All the storms are greater than 60 km away, so in this range, the height used is an under estimate and the difference is 500-1000 m. The 6 June 2005 storm was 89 km from the radar making the difference in height close to 1 km.

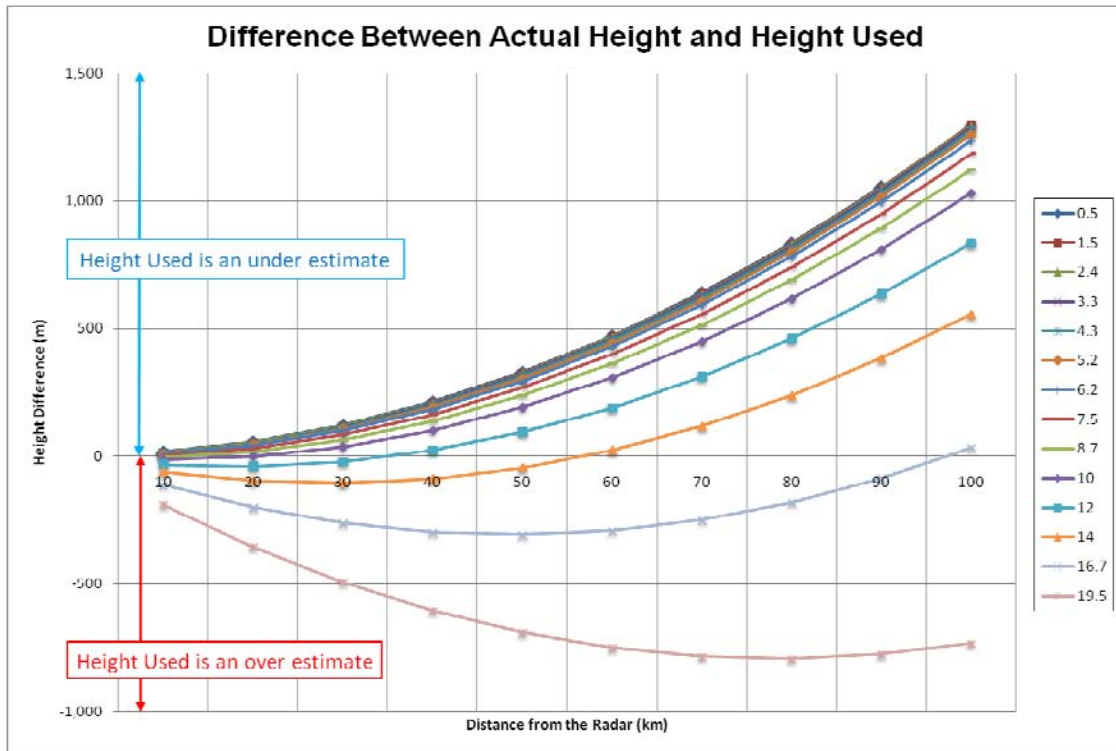


Figure 13. Differences between Height used and Actual Height. Height differences greater than zero are an under estimate for the height used. Height differences less than zero are an over estimate for the height used.

The height used to position the elevation angle was also used in the vertical reflectivity plot. Using the actual height would redistribute the placement of the reflectivity data point and the spline would look similar but the sampled area, -10°C to -40°C , would include a different section of the spline. The adjusted spline would then greatly affect the LVIF calculation.

B. FUTURE RESEARCH

While this study expected certain limitations from the beginning, the impacts of these limitations were minimal. However, unexpected limitations were encountered: time frame, missing lightning data, depth of storm on the radar. Correcting for these errors, LVIF could still provide profitable results. Previous research (i.e., Gauthier et al. (2006) and Carey and Rutledge (2000)) had positive indication that ice mass correlates to flash density and flash rate, respectively. Forecasting lightning onset from ice content has good theory behind it but requires more data than was available to this study. The

vertical plot was a sound tool for stronger storms. A more robust storm sample is necessary for statistical analysis to determine a trend of ice content. Currently, the 45 WS is installing a dual-polarized radar. Future developments in the LVIF approach using this new technology may provide further insight into lightning forecasting.

LIST OF REFERENCES

- Air Force Combat Climatology Center. [available online at
<https://notus2.afccc.af.mil/SCISPublic/services/databases.asp>.]
- Carey, Lawrence D. and Steven A. Rutledge, 2000: The relationship between precipitation and lightning in tropical island convection: A C-Band polarimetric radar study. *Mon. Wea. Rev.*, **128**, 2687-2710.
- D'Arcangelo, D.L., 2000: Forecasting the onset of cloud-ground lightning using layered vertically integrated liquid water, M.S. thesis, Dept. of Meteorology, Pennsylvania State University, 60 pp.
- Doviak, Richard J. and Dušan S. Zrnić, 1993: *Doppler Radar and Weather Observations*. 2nd ed. Academic Press, INC, 562 pp.
- Dye, James E. and John C. Willett, 2007: Observed enhancement of reflectivity and the electric field in long-lived Florida anvils. *Mon. Wea. Rev.*, **135**, 3362-3380.
- Gauthier, Michael L., Walter A. Petersen, Lawrence D. Carey, and Hugh J. Christian Jr.. 2006: Relationship between cloud-to-ground lightning and precipitation ice mass: A radar study over Houston. *Geophysical Research Letters*, **33**.
- Global Hydrology Resource Center, cited 2008: Lightning Detection and Ranging (LDAR) Dataset Summary [Available online at:
<http://ghrc.msfc.nasa.gov/uso/readme/ldar.html>.]
- Greene, Douglas R. and Robert A. Clark, 1972: Vertically integrated liquid water—A new analysis tool. *Mon. Wea. Rev.*, **100** 548-552.
- Hodanish, Stephen, David Sharp, Waylon Collins, Charles Paxton, and Richard E. Orville, 1997: A 10-yr monthly lightning climatology of Florida: 1986-95. *Wea. Forecasting*, **12** 439-448.
- Huffines, Gary R. and Richard E. Orville, 1999: Lightning ground flash density and thunderstorm duration in the continental United States: 1989-96. *J. Appl. Meteor.*, **38**, 1013-1019.
- Kuettner, Joachim P., Zev Levin, and J. Doyne Sartor, 1981: Thunderstorm electrification—Inductive or non-inductive? *J. Atmo Sci.*, **38**, 2470-484.

- Lambert, Winifred, David Short, Matthew Volkmer, David Sharp, and Scott Spratt, 2007: Using flow regime lightning and sounding climatologies to initialize gridded lightning threat forecasts for East Central Florida. Preprints, *16th Conf. on Applied Climo.*, San Antonio, TX, Amer. Meteor. Soc., P2.1.
- Marshall, J. S., and W. McK. Palmer, 1948: The distribution of raindrops with size. *J. Meteor.*, **5**, 165–166.
- Meridian World Data, cited 2008: Distance Calculation [Available online at: <http://www.meridianworlddata.com/Distance-Calculation.asp>.]
- National Climate Data Center, cited 2008: HDSS Access System. [Available online at: <http://hurricane.ncdc.noaa.gov/pls/plhas/HAS.FileAppSelect?datasetname=6500>.]
- National Weather Service, cited 2008: Distance Learning Operations Course Topic 3: Principles of Meteorological Doppler Radar, Lesson 1: WSR-88D Fundamentals [Available online at: <http://www.wdtb.noaa.gov/courses/dloc/topic3/lesson1/index.html>.]
- Peterson, Walter A. and Steven A Rutledge, 2001: Regional variability in tropical convection: Observations from TRMM, *J. Clim.*, **14**, 3566-3586.
- Rinehart, Ronald E., 1997: Radar for Meteorologists 3rd ed. Knight Printing Company, 428 pp.
- Roeder, William P., Todd M. McNamara, Billie F. Boyd, Johnny W. Weems, and Stephen B. Cocks, 2005: Unique uses of weather radar for space launch. Preprints, *32nd Conf. on Radar Meteor.*, Albuquerque, NM, Amer. Meteor. Soc., P8R.13.
- University of Wyoming, cited 2008: Database of Worldwide Atmospheric Soundings [Available online at: <http://weather.uwyo.edu/upperair/sounding.html>.]
- Weems, Johnny W., Clark S. Pinder, William P. Roeder, and Billie F. Boyd, 2001: Lightning watch and warning support to spacelift operations. Preprints, *18th Conf. on Wea. Ana. and Forecasting*, Fort Lauderdale, FL, Amer. Meteor. Soc., P4.16.

INITIAL DISTRIBUTION LIST

1. Defense Technical Information Center
Ft. Belvoir, Virginia
2. Dudley Knox Library
Naval Postgraduate School
Monterey, California